

# Size-Resolved Characterization of Particles and Fibers Released during Abrasion of Fiber-Reinforced Composite in a Workplace Influenced by Ambient Background Sources

**Kling, Kirsten I.; Levin, Marcus; Jensen, Alexander C. O.; Jensen, Keld A.; Koponen, Ismo K.**

*Published in:*
Aerosol and Air Quality Research

*Link to article, DOI:*
10.4209/aaqr.2015.05.0295

*Publication date:*
2016

*Document Version*
Publisher's PDF, also known as Version of record

*Aerosol and Air Quality Research*, 16: 11–24, 2016

ISSN: 1680-8584 print / 2071-1409 online
doi: 10.4209/aaqr.2015.05.0295

# Size-Resolved Characterization of Particles and Fibers Released during Abrasion of Fiber-Reinforced Composite in a Workplace Influenced by Ambient Background Sources

**Kirsten I. Kling[1*], Marcus Levin[1,2], Alexander C.Ø. Jensen[1], Keld A. Jensen[1], Ismo K. Koponen[1]**

[1] *National Research Centre for the Working Environment, 2100 Copenhagen, Denmark*
[2] *Department of Nanotechnology, Technical University of Denmark, 2800 Kgs. Lyngby, Denmark*

## ABSTRACT

We demonstrate the use of high- to low-resolution microscopy and particle chemical analysis during normal vacuum and cryo-conditions to identify the nature and relative abundances of process-generated particles and fibers from sanding of a glass and carbon fiber epoxy layer-composite in a workplace influenced by both indoor and ambient background sources. The study suggests that a proper exposure characterization requires multiple techniques covering wide size ranges to reach a conclusion. Besides a rise in number concentration due to release of particles during the sanding, a significant contribution of ambient particles to the background in the production facility was observed in the sub-micron size range. Fibers are posing a dominant exposure risk in the micron size range, with carbon fibers dominating in count.

***Keywords:*** Fiber mats; Particle identification; Epoxy; Production emission; HR-TEM.

## INTRODUCTION

Epoxy composites have several applications, especially in high performance lightweight products where high strengths and durability is required. Applications include certain parts of cars, boats, aircrafts and windmills where the mechanical load to the material may require use of increased strength and durability. Fibers and fiber mats are well known for adding strength and durability to composite materials. However, the concern is that manufacturing of fiber-reinforced composites also inherently involves the potential risk of fiber exposure as it has been known for decades that processing composites (e.g., reparing, grinding, cutting and drilling) may generate dust and fibres in the respirable size range (Midtgård and Jelnes, 1991). The first laboratory studies found that sanding of fibre-reinforced composites as well as sanding machinery emit high amounts of ultrafine nanoparticles (Zimmer and Maynard, 2002; Koponen *et al.*, 2009, 2011; Gomez *et al.*, 2014). Bello *et al.* (2009) also found that dry cutting of alumina and carbon fibre-reinforced composites produced submicron rod like fibres. Previous studies have shown that reworking of composites with engineered nanomaterials embedded in the matrix do not release free engineered nanoparticles, the released fragments show that the filler is not separated from the polymer matrix (Koponen *et al.*, 2011; Wohlleben *et al.*, 2011; Gomez *et al.*, 2014).

It may be anticipated that the potential for fiber release is strongly related to the fiber characteristics and the structure of the composite. Matrix composites would be expected to be associated with lower potential for fiber release than in the case of layer composites and composites with matrix-embedded fibers at the surface of the product. Opposite brittle fibers are thought to break up easily and would become more fragmented during mechanical treatment as compared to strong and highly durable fibers. Thus it is also of interest to investigate the types of fibers potentially released from such processes. Fibres (SiC, Skogstad *et al.*, 2006) represent a probable cause for the observed increased occurrence of lung diseases among workers in the Norwegian Silicon Carbide Industry (Føreland *et al.*, 2008: Bugge *et al.*, 2012; Johnsen *et al.*, 2013).

Due to their characteristics (morphology and material dependent biopersistens), fibers are known to have adverse health effects when inhaled (e.g., Lippmann, 1990a, b; Hesterberg *et al.*, 1996; Donaldson and Tran, 2004).

The contribution of particles from background sources is one of the major challenges in the interpretation of continuous real-time measurements in workplace studies. A common approach is to use online measurements with two or more high time-resolution measurement devices simultaneously by which the major near and far-field sources can be distinguished (e.g., Jensen *et al.*, 2015;

[*] Corresponding author.
Tel.: +45 39165365; Fax: +45 39165201
*E-mail address:* kirstenlieke@gmx.de

Kaminski *et al.*, 2015; Koivisto *et al.*, 2015). However, such measurements are still challenged by the fact that the different airborne particles and their sources are not unequivocally identified. Consequently, further analyses are often required to characterize and quantify the exposure in greater detail. Currently, there is a consensus that the best approach to assess the exposure to engineered nanomaterials in workplaces is represented by the nanoparticle emission assessment technique (NEAT, Methner *et al.*, 2009, 2010) applying instruments measuring the number concentrations of the nanomaterials together with filters (or other sampling techniques) that allow offline analysis of samples for particle (mass,) morphology, size, count, and elemental composition (adopted from Savolainen in Vogel *et al.*, 2013, changes in parenthesis). One of the greatest challenges is discrimination between different factory (primary) emissions and the outdoor background, which enter through mechanical ventilation and other more or less controlled ventilation paths in the workplace (e.g., Ono-Ogasawara *et al.*, 2009; Ramachandran *et al.*, 2011; Koivisto *et al.*, 2015). The characteristics and composition of this outdoor contribution may vary considerably from place to place and over time depending on the location and outdoor activities. A review by Kuhlbusch *et al.* (2011) summarises the importance of this discussion.

In this study we focus on identifying and characterizing the potential release from a glass/carbon fiber (Si/C-fiber)-reinforced layered epoxy composite. We aimed to observe particles related to the processing (sanding) of the composite as well as particles present in the background air of the production site. We demonstrate the use of different microscopy techniques and particle chemical analysis to identify the nature and relative abundances of particles and fibers collected from ambient air and deposited dust in the vicinity to sanding and cutting of a glass and carbon fiber-epoxy layer-composite. Furthermore, we identify the influence of an ambient background source and characterize these beam sensitive particles by Transmission Electron Microscopy (TEM) and chemical analysis under cryo-conditions. We apply Scanning Electron Microscopy (SEM) on the deposited sanding debris considered to be highly abundant in large particles, and find significant amounts of fibers in the micron size range. Furthermore, we collected fibers on filters for optical microscopy, enabling us to directly distinguish between carbon and glass fibers in this size range.

The study demonstrates that a proper particle characterization and discrimination of sources easily requires multiple techniques to cover wide size ranges to reach a conclusion. This is also particularly important for exposure specific administrative use of occupational measurement data. We therefore focus on the nature of both, the nanoscale particles and the fibers released in the micron and above micro meter size range.

## MATERIALS

This study was conducted as part of a large study to investigate the release of dust and fibers during different procedures of sanding and cutting an industrial prototype glass/carbon fiber (Si/C-fiber)-reinforced layered epoxy composite (Jensen *et al.*, 2015). The composite material was made from a two part layering, and reinforced with glass and carbon fibres (Devolt AMT, Langevåg, Norway). The first part of the layer is containing 30–40% carbon fibres and 60–70% glass fibres and the second part of the layer is a fibre fabric consisting of 19.5–30% carbon fibre, 39–52.5% glass fibre, and 25–35% polyamide/polypropylene matrix. The second layer makes up to 65–75% of the composite material in mass. In the sanding process, the two layers are sanded at the same time and cannot be differentiated for emissions.

## METHODS

Measurements were performed in a production hall located in a rural area, with farming activities going on occasionally.

Si/C-reinforced epoxy composite parts were sanded using an Atlas Copco Grinding GTG21 angle grinder (8500 RPM) and an Atlas Copco LST 31 random orbital sander (9000 rpm). In addition, an APK type NAG11A -05 (880 W) was used to saw the test material. All machines were pneumatic and equipped with local exhaust suction connected to a main exhaust system. The maximum velocity in the machine exhaust was 34 m $s^{-1}$ measured from the end of the tube with a vane probe (435, Testo). Sanding was repeated three times for 10 minutes. The used sandpapers' grit sizes (ISO 6344 standards), suppliers, abrasive material and referring particle diameter (μm) of sandpaper used in this study are given in Table 1. Sandpaper has significantly larger grain sizes than the dust investigated in this study and can thus be excluded as a source in the analyses. Cutting was conducted by cutting slices from the composite. Cutting was done two times for 12 minutes.

### *Particle Monitoring*

Continuous real-time measurements were completed using an ELPI+ (Electric Low Pressure Impactor; ELPI+, Dekati Ltd., Finland) and a Condensation particle counter (CPC, Model 3007, TSI Inc., Minnesota, USA) to derive

**Table 1.** The grit sizes (ISO 6344 standard), suppliers, abrasive material and referring particle diameter (μm) of sandpaper used in this study.

| Grit designation (ISO 6344) | Manufacturer | Material | Avg. particle diameter (μm) |
|---|---|---|---|
| P24 | VSM, Germany | $Al_2O_3/ZrO_2$ | 764 |
| P36 | Sia, Switzterland | SiC | 538 |
| P40 | Klingspor, Germany | $Al_2O_3$ | 425 |
| P60 | Klingspor, Germany | $Al_2O_3$ | 269 |

aerosol particle concentrations and size distributions in the working area. The ELPI+ measures the aerodynamic size of particles and calculates their size-resolved concentrations based on size-fractionated aerosol charge. In this work, we assume that the aerosol has a unit density throughout the measurement scale.

### *Dust Sampling*

Three different types of particle samples were collected for different electron microscopy (EM) techniques and optical microscopy (OM).

*Samples for Transmission Electron Microscopy*

Short term high-efficiency aerosol samples for TEM were collected near the working area using a Micro INertial Impactor (MINI, Kandler, 2009). The sampling time was set approximately from 30 seconds to one minute with focus on collecting particles from the sanding events for detailed electron microscopy analysis. The sampling times are indicated by the cyan coloured underline in Fig. 1(a). Sampling was performed on 2 stages (with a $d_{50}$ cut-off at 0.05 and 0.9 μm aerodynamic diameter, respectively) on Ni-TEM grids with Formvar carbon foil (Plano, Germany). A diaphragm gas pump (NMP 830, KNF Neuberger, Germany) ensured a flow of 0.5 L $min^{-1}$.

*Samples for Scanning Electron Microscopy*

We collected deposited materials from surfaces at the working site for analysis with SEM. Material was gently brushed from the treated composite after sanding took place, and placed in clean plastic bags. The bags were sealed and stored in darkness until analysis. For analysis, material was dripped on to silicon wafers and adhesive carbon substrates, and gently blown off; in addition, stubs were also dipped in the bulk and on to the walls of the plastic bags, to ensure that both coarse and fine particles were collected.

*Samples for Optical Microscopy*

Dedicated fiber samples were collected as indicated in Table 3 on person ("Personal") and stationary near-field ("Central"), far-field ("Background") and environmental background ("Outdoor") using 3-piece polystyrene monitors, known to be used for asbestos sampling, mounted with 25 mm, 0.8 μm pore size, OD MF-Millipore membrane filters (Merck KGaA, Germany). Sampling was maintained at 1.7 L $min^{-1}$ using personal sampling pumps (APEX, Casella, Illinois, USA).

After sampling, the inlet and outlets of the filters were closed, and the entire sample stored in darkness until needed for analysis. Optical microscopy analysis was made only on the filter pieces from the asbestos sampler, mounted on clean frosted glass microscope slides (25 × 75 mm) and made transparent according to the NIOSH 7400 procedure using an acetone vaporizer (Small Wonder Acetone Vaporizer, Wonder Makers Environmental, Michigan, USA).

### *Classification of Particles Using the "Groupp" Classification Scheme*

"Groupp" is a classification scheme presented by (Kandler *et al.*, 2011) that sorts single particles into mineral groups based upon chemistry and morphology data derived by SEM/EDS in electron microscopy. It has been applied on mineral dust emissions and pollution particles in atmospheric aerosol samples. In this study, we apply it on data derived by automated single particle analysis SEM/EDS and use the same nomenclature and classification criteria for data derived by TEM manually (including EDS and EELS).

### *Transmission Electron Microscopy Analyses*

TEM was used for analysis of particles on 12 impactor TEM samples from 6 tests in total. Overview and high-resolution (HR) images were recorded using a Tecnai T20 G2 (FEI, The Netherlands) operated at 200 kV.

Because of some of the collected particles were beam-sensitive, a nitrogen cooled cryo transfer holder (Gatan Inc., California, USA) was used to keep the sample at –180 degrees Celsius during analysis. Hereafter, we will refer to this procedure as Cryo-TEM. For imaging, it was attempted to reduce beam damage and hydro carbon deposition on the collected particles by analysing the samples at low beam current densities and short acquisition times. Energy dispersive X-ray detection (EDS) was carried out on single particles in the TEM using an Oxford 80 mm silicon drift detector. Electron energy loss spectroscopy (EELS) was carried out on single particles using a GATAN 965 GIF Tridiem (Gatan Inc., California, USA).

Particles in the size range from approximately 50 nm up to 500 nm (projected area diameter) on TEM grids were analysed and classified based on their structure (derived by high-resolution and electron diffraction), morphology, beam stability and chemical composition (derived by EDS and EELS). The results are interpreted using the "Groupp" classification scheme.

### *Scanning Electron Microscopy Analyses*

Deposited dust samples were analysed by SEM using an Environmental SEM Quanta 200 FEG and a Helios Nanolab FIB-(Focused Ion Beam) SEM (both FEI, The Netherlands), both equipped with an energy dispersive X-ray analyser (EDS).

Automated single particle analysis was applied using the EDAX (New Jersey, USA) Genesis software and manual post-processing as described in (Kandler *et al.*, 2011). Spiral matrixes of 10 × 10 adjacent fields at magnification 2000× were placed in the center of each sample. The particle area is evaluated by summing all the pixels within the particle, the average diameter defined as the diameter of a circle with the same area. For automated classification of the particles, the "Groupp" classification scheme is used. In order account for the different chemical contributions from the substrates (C vs. Si), background correction was applied in the SEM before analysis on each substrate (adhesive carbon substrate and silicon wafers). In addition, measurements of C and morphological criteria are taken into account when manually post-processing the automated data. Except for the background subtraction, this process does not differ from the method used in (Kandler *et al.*, 2011) and (Lieke *et al.*, 2011). The classified particles are finally summarized into

groups (Table 2) and displayed in diagrams of size resolved relative number abundance (see results, Figs. 2 and 4), where *n* is the number of analysed particles for each size interval.

***Optical Microscopy Analysis***

Optical microscopy was conducted using a Leica DM IL optical microscope (Leica Microsystems Wetzlar GmBH, Germany) mounted with a Nikon DS-Fi2 digital camera (Nikon Instruments Europe B.V, Nikon Group, Japan). Images were collected using this camera and a Nikon Digitial Sight DS-U3 interface and processing using the NIS Elemements v 4.11. The microscope was mounted with 4 objective lenses with objective lens magnifications of 4, 10, 20 and 32.

**Table 2.** Chemical grouping criteria for automated single particle analysis in SEM and manual TEM analysis based on the classification scheme of Kandler *et al.* (2011).

| Group | Group after Kandler *et al.* (2011) | Additional morphological characterisation |
|---|---|---|
| Soot (on TEM samples only) | Soot | Complex aggregates, onion shell-like structure |
| Soot mixture (on TEM samples only) | Soot + Ammonium sulphate | Round shaped attached to complex aggregates |
| Environmental contribution | biological | Rests of vegetation, spores |
| | Na-rich | |
| | Ammonium sulphate** | Round shaped, d = ~50–350 nm |
| | Na sulphate | ** on TEM samples only |
| | Other sulphate | |
| | Ca carbonate | |
| | Ca Mg carbonate | |
| | Phosphate | |
| | Na chloride | |
| | K chloride | |
| | Mixtures Cl+S | |
| | Other K-dominated | |
| | Other Ca-dominated | |
| Si and mixtures | Quartz* | * background corrected (on Si substrate) |
| | SiAl* | |
| | SiAlK* | |
| | SiAlNa* | |
| | SiAlNaCa* | |
| | SiAlNaK* | |
| | SiAlCaFeMg* | |
| | SiAlKFeMg* | |
| | SiAlFeMg* | |
| | AlSiNaCa* | |
| | AlSiMgFe* | |
| | SiMgFe* | |
| | SiMg* | |
| | SiCaTi* | |
| | Mixtures Si+S* | |
| | Mixtures AlSi+S* | |
| | Mixtures NaCl+Si* | |
| | Mixtures NaCl+AlSi* | |
| | Mixtures Ca+Si* | |
| | Mixtures Ca+AlSi* | |
| | Other Si-dominated* | |
| C dominated dust/epoxy | Soot* | * background corrected (on C substrate) |
| | Soot | No size limitation, not fulfilling soot morphological characteristics |
| | Si-groups above, if more than 80 wt% C were measured on Si-substrate | |
| Metal Oxides and steel | Fe oxide | |
| | Ti oxide | |
| | Al oxide | |
| | Steel | |
| No group | Other Mg-dominated | |
| | Other | |

## RESULTS

### *Particle Monitoring*

Online particle measurements demonstrated clear particle release events during sanding (Fig. 1(a)). The release resulted in numerous short term peak-durations ranging from seconds to a few minutes of which some reached peak concentrations exceeding $2.2 \times 10^5$ cm$^{-3}$. The analysis of the on-line size-distribution measured with the ELPI+ indicates that on average, the released particles are found in the entire size-range measured i.e., from ca. 6 nm to 10 µm (Fig. 1(b), black). However, when comparing total number concentration size distribution data during sanding and pre-activity, it shows that almost no sanding particles are generated in the intermediate size range of ca 200–300 nm (Fig. 1(b), pre-activity indicated in red). Cutting (not shown) did not show any increase in number concentration.

### *Dust and Particle Samples*

*Analyses of TEM Samples*

MINI impactor sampling periods are indicated in Fig. 1(a) by cyan coloured underlines. No significant difference is observed between the samples at different sanding events (cutting was not sampled); therefore results are summarized for all TEM samples in the following section and respective Figures.

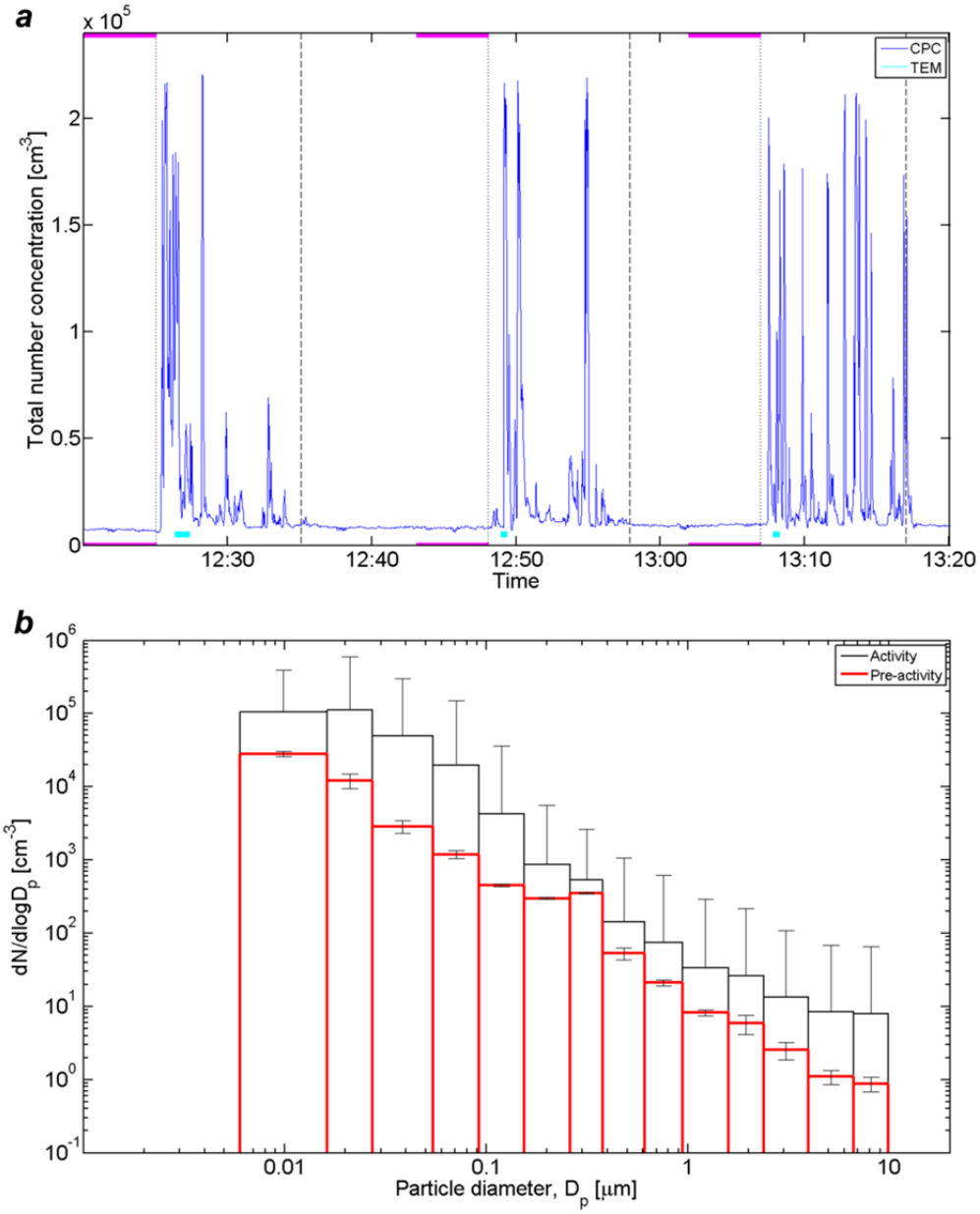


**Fig. 1.** a) CPC online measurement showing clear particle release events during grinding and b) ELPI particle size distribution averaged over the grinding events (black, indicated by the frames given by the dashed lines in the CPC time line, x-axis upper panel) and background (red, underlined in purple in the CPC time line, x-axis upper panel). Cyan coloured underlines mark the TEM sampling.

The classification of particles on the TEM samples is based on morphology, crystal structure and, if available, chemical analysis by EDS and EELS and follows the scheme and evaluation in Kandler *et al.* (2011), Lieke *et al.* (2011) and Lieke *et al.* (2013). Results in relative number abundance of particles groups in the size intervals 50 to 100 nm, 100 to 250 nm and 250 to 500 nm are shown in Fig. 2. We refer to "environmental contribution" for particles believed to stem from outside the production hall and being transported into the hall through the ventilation system and open doors and windows. We expect to find sanding debris of the composites including breakdown material of fibers to be dominated by either C or Si, and named the groups accordingly "Si and mixtures" (allowing for a broader chemical composition) and "C dominated". Examples of particles in approximately this size range are displayed in Fig. 3. Despite the high number concentration measured by the online instruments in the events, particles allocated to the sanding of epoxy (Figs. 3(a) and (b)) are less abundant on the TEM samples, i.e., in this size range. As displayed in Fig. 2, the C dominated particles are hardly represented in the size intervals below 250 nm, and account for only 5% of the particles in the size interval above. The glass fiber component makes only 2% of the collected particles.

The TEM samples do, however, reproduce the dominant background presence of particles around 200 nm, as indicated by the size distribution (Fig. 1(b)). Our analysis reveals a high relative number abundance (Fig. 2, "environmental contribution" up to 80%) of spherical particles (Figs. 3(d) and 3(e)), predominantly around 200 nm. Based on their chemical composition, shape and beam stability and interpreted with the classification scheme, these particles may be classified as ammonium sulfate (or particles dominated by ammonium sulfate). The nature of the 200 nm ammonium sulfate bearing particles is further investigated in Cryo-TEM at –180°C. These particles which in normal TEM appear as homogeneous, droplet like, spherical particles (Fig. 3(e)) show a phase separation (Fig. 3(f)) of crystallized ammonium sulfate surrounded by an amorphous, carbonaceous material. We here make use of the mechanism called efflorescence, which is due to solution chemistry between ammonium sulfate and organic compounds and/or water in the aerosol droplet (e.g., Imre *et al.*, 1997; Cziczo and Abbatt, 1999; Bertram *et al.*, 2011).

Soot particles (Fig. 3(c)) are identified based on their complex morphology and onion shell-like graphitic structure (e.g., Wentzel *et al.*, 2003; Lieke *et al.*, 2011, 2013). Those are found in abundances of 5 to 10% (Fig. 2, "soot"). Some few of the soot particles in the larger size intervals are attached to ammonium sulfate particles (Fig. 2, "soot mixture", 1–3%). It must be noted that ammonium sulfate particles never include or cover soot or other particles fully: In this study, "soot mixture" refers to attachments of soot to ammonium sulfate particles.

Metal oxides as for example iron oxide rods (Fig. 3(h)), titanium (di)oxides, aluminium oxides and steel particles appear in all sizes.

Single fibers of some tens of nm width and some hundreds of nm in length are found on the TEM samples (Fig. 3(g)) as well. A few ca 20 nm thin fibers are found in larger agglomerates of few hundred nanometers, with the fibers sticking out of the bulk (see also Jensen *et al.*, 2015).

Ca 6% of the particles in the TEM samples cannot be allocated to one of the above-mentioned particle groups due to the sharp classification criteria. Some of them might be mixtures of more than two groups. However, these particles are not forming their own group, as they are different from each other in terms of chemistry and morphology. This concerns 65 particles in total.

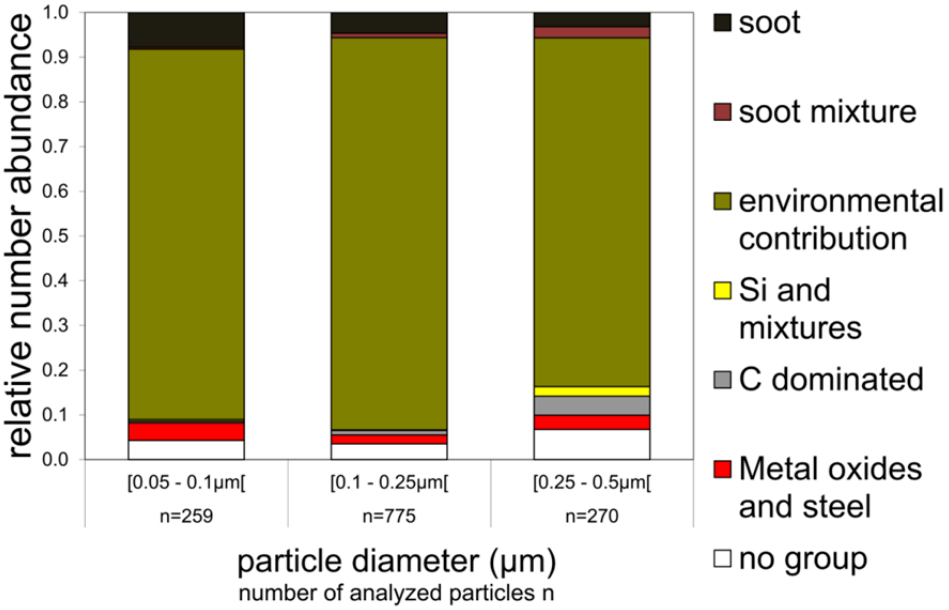


**Fig. 2.** Relative number abundance of particles groups for the TEM samples. Here, "environmental contribution" refers mostly to particles classified as ammonium sulfate by their shape, chemical composition and beam stability.

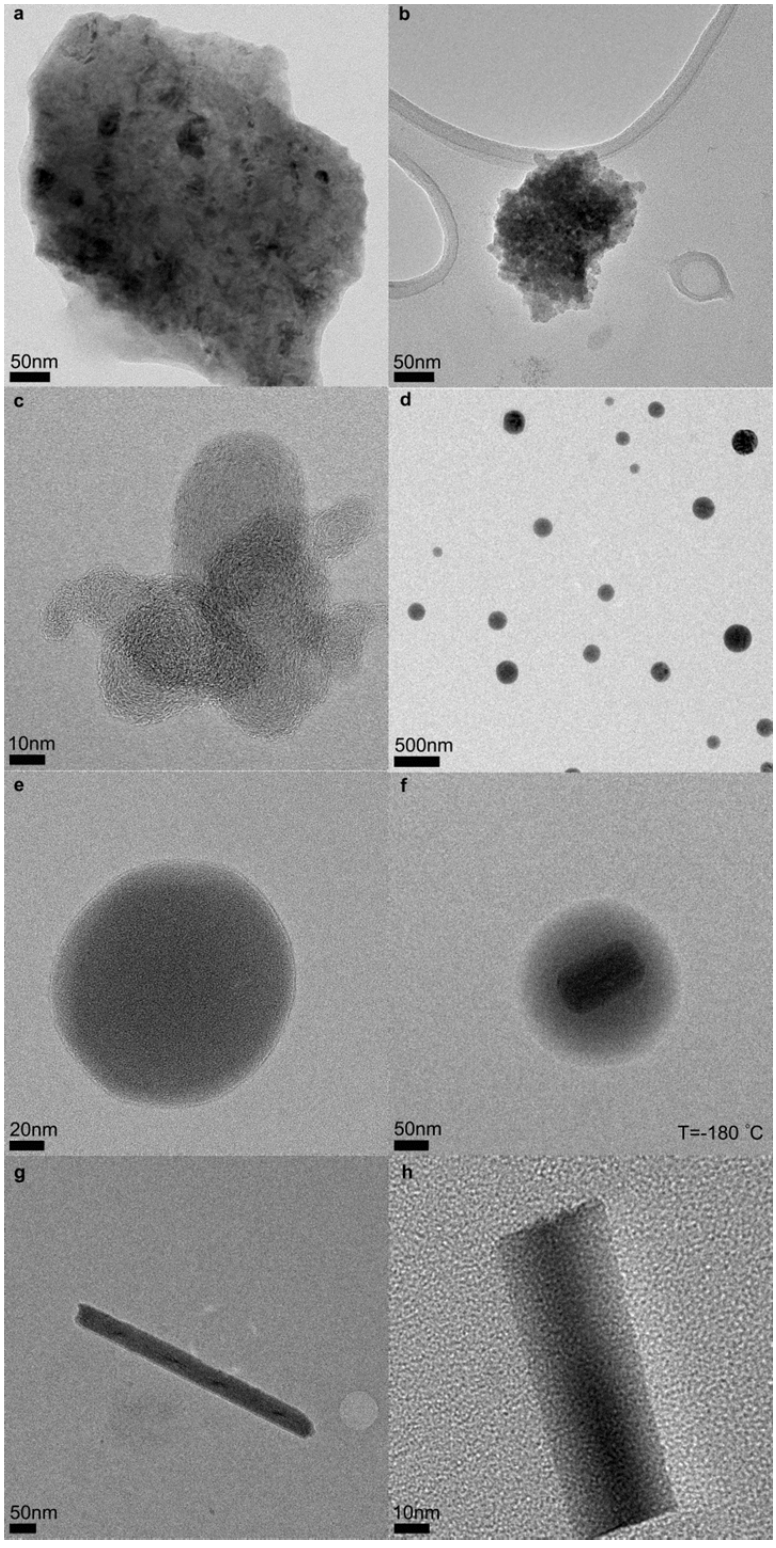


**Fig. 3.** Examples of particles from the TEM samples. a) carbonaceous particle with parts of crystallized epoxy; b) C-dominated particle; c) soot; d+e) particles classified as ammonium sulfate based on their shape, chemical composition and beam stability; f) same at -180 degrees C; g) nano scale fiber; h) Iron oxide rod. HRTEM bright field images obtained

*Analyses of SEM Samples*

The quality of the SEM samples was sufficient for automated single particle analyses. The results of all samples are combined in Fig. 4. Examples of particles observed on these samples by SEM are displayed in Fig. 5.

Figs. 4 and 5 illustrate that the majority of particles allocated to sanding of the composite material is present in the micron size range. The deposited dust is dominated by

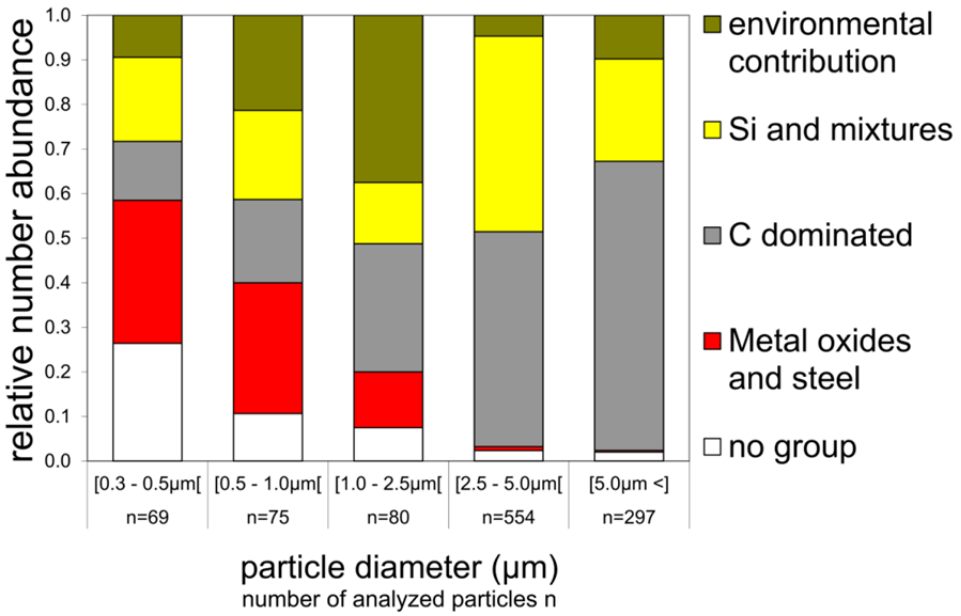


**Fig. 4.** Relative number abundance of particles groups for the SEM samples of deposited dust summarized into the groups after automated classification. Here, "environmental contribution" refers to groups given in table 2, except for ammonium sulfate.

irregular shaped C and Si bearing particles and fibers. Abundance to these (composite and filler) materials in the deposited sanding dust increases significantly with increasing particle size. Together, the C and Si rich groups constitute approx. 90% in the size range above 2.5 µm ("Si and mixtures", "C-dominated", Fig. 4). This is also in good accord with observations from the OM analysis of the fiber filter samples (see images in Table 3).

A significant contribution of material from the ambient atmosphere can be observed by the abundance of e.g., potassium and calcium bearing material ("environmental contribution", Fig. 4). This group peaks around 1 µm, likely biased by sea salt and sulfate bearing particles.

Metal (Al, Fe, Ti) oxides and steel particles are expected to partially enter from the ambient air pollution, but chemically similar types of particles are likely originating from machinery wear and are abundant in the deposited dust. They are found predominantly in the sub-micron size range.

Particles that cannot be allocated to the above-mentioned sources are classified as "no group". The high abundance of that group is due to the sharp cut-off of the original classification and technical difficulties in analysing small particles on top of the substrates' background. The chemical composition within that group is very broad, no overall trend is observed and most particles are thus suspected to be mixtures of two or more groups, thus disqualifying for classification. The mixing is likely secondary and due to agglomeration during storage, and thus not relevant for exposure. For larger particles, the abundance of this group drops significantly, as large particles are dominating the bulk chemistry of mixtures.

It must be noted that SEM investigations on the deposited material reveals extreme charging of particles, especially of the fibrous material, leading to the conclusion that this material has lower electrical properties. However, non-fibrous particles originating from the composite prove to be partly crystalline material, likely epoxy crystals. Small particles seem to cluster around larger individual particles. From the images (e.g., Figs. 5(a)–5(d)) it can be concluded that mixing occurs in any size range.

Particles with aspect ratios above 3 (fibers) are predominantly found in the groups "Si and mixtures" and "C dominated" in the size range above 2.5 µm. Particles with aspect ratios above 3 account for 2% of the analysed particles in the size range 2.5–5 µm, increasing to 16% of the size range above 5 µm in the automatically analysed samples (e.g., Figs. 5(c) and 5(d)). Material coarser than 100 µm size (Figs. 5(e) and 5(f)) is fibrous, which is also in agreement with the OM data. Fibers classify either as "Si and mixtures" or as "C dominated". There seems to be no obvious morphological difference between carbon and silica-based fibers and no chemical difference is observed as function of size.

Figs. 5(d), 5(e) and 5(f) also show that fibers in this study are mainly rod-shaped and straight, rather than curved. Given a sufficient thin dispersion over the sampling substrate, they are rather occurring single than agglomerated, i.e., agglomeration is believed to stem from overlaying of particles on deposition on the sampling substrate.

In this size range, fibres do clearly not stick or are embedded in the composite matrix.

*Analysis of Filter Samples with OM*

The analysis shows that the filters collected during sanding activities (indicated in Fig. 1(a)) contain a significant number of fibers and fine to coarse µm-sized particles at all three indoor locations (Table 3). The fibers are dominated by opaque carbon fiber fragments and a lower abundance of

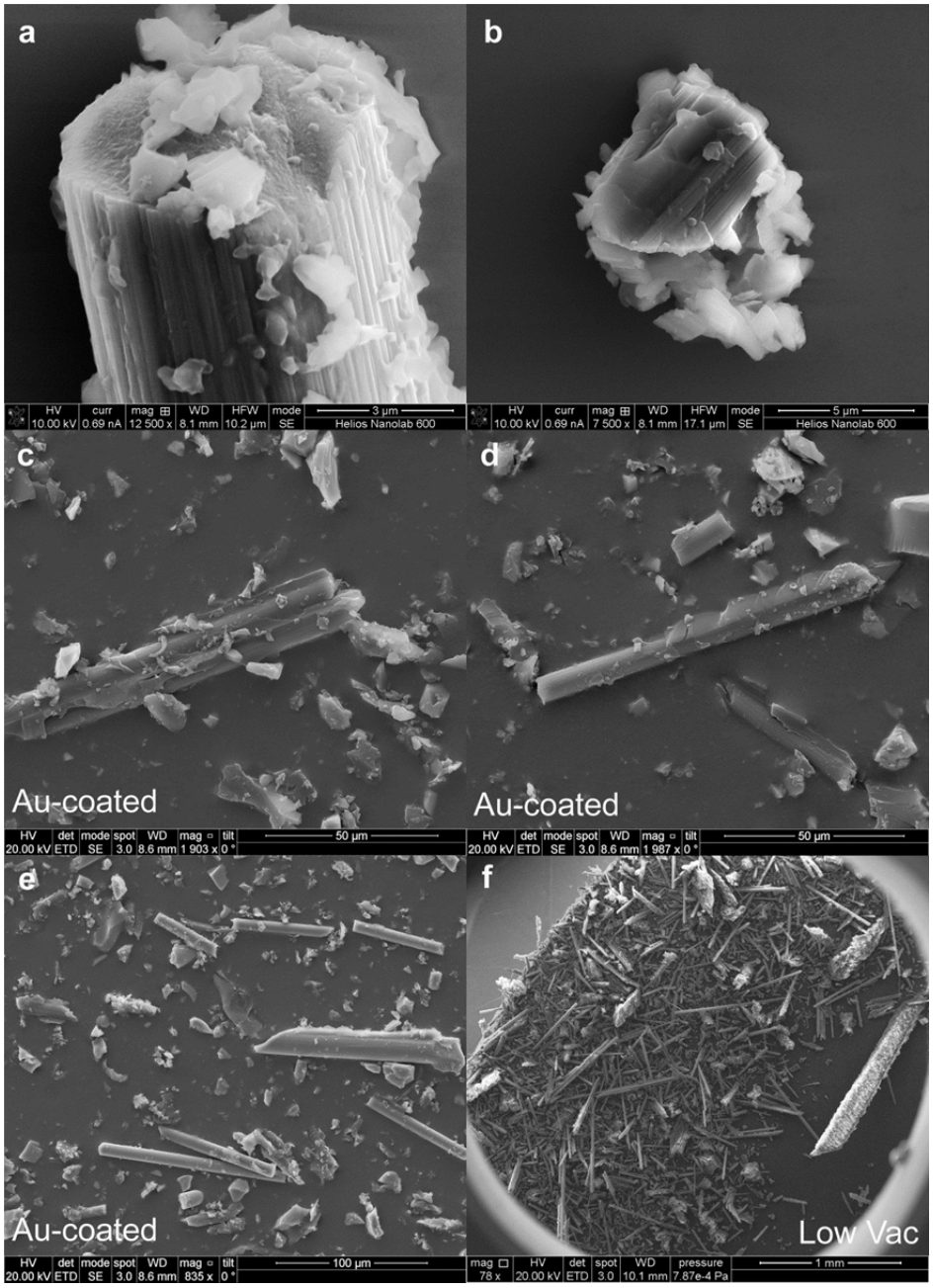


**Fig. 5.** Examples of particles from the SEM samples, deposited dust. a) top end of silicon fiber; b) breakdown part of silicon fiber; c and d) fibers and particles in the µm range; e) large fibers and particles of various geometry; f) macroscopic view on the sample showing the increased abundance of fibers.

transparent fibers, which is the appearance of glass fiber (e.g., "A7" and "A5" in Table 3). In addition to the carbon and glass fibers, a few irregular bulky and thread like fiber-like materials are also observed (e.g., "A17" and "A3" in Table 3) and may be biogenic and textile fibers, respectively. The coarser particle shaped material is usually dominated by transparent (glassy-like) particles and mixtures with i.e., opaque compounds. In this case, this glassy compound is assumed to be the epoxy matrix in the composite, and is also observed partially adhered to some of the carbon fibers. In a few cases, entire fragments of a few fibers associated with this glassy matrix are observed.

The sample collected during cutting (sawing) is dominated by mainly transparent particles and a minor fraction of relatively short fiber fragments. Hence, due to this difference from the sanding dust, there appears to be a difference in the exposure characteristics between cutting and sanding, where cutting appeared to result in much lower release of fibers.

For comparison, the outdoor reference sample only shows presence of a few small opaque fibers and coarser irregular "biogenic" bulky fibers as mentioned above. Consequently, the outdoor samples strongly indicate that there are no important outdoor sources to the fibers and other coarse-fraction particles in the outdoor surroundings.

**Table 3.** Summary results from the optical microscopy analysis of dust collected using the fiber sampler.

| Filter | Image (900 µm width) | Position | Sampling time [min] ($m^3$ air) | Process | Local Exhaust Ventilation | Optical microscopy observations |
|---|---|---|---|---|---|---|
| A1 $\times 10^{-1}$ |  | Central | [36] (0.0612) | 20 min Sanding HEV12020 1 min Vacuum cleaning | NA | A few glass and carbon fibres (n = 0.6/image) with short to intermediate lengths and numerous opaque and transparent dust particles were observed. Fibres resembling biogenic material were also observed. |
| **A2** $\times 10^{-1}$ | 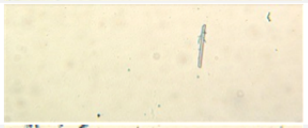 | Personal | [33] (0.0561) | | Yes - 20 min No - 1 min | **Some long fibres and numerous opaque and transparent dust particles were observed. Relatively, carbon fibers were much more abundant than silica fibres (> 90%; n = 2.5/image).** |
| A7 $\times 10^{-4}$ | 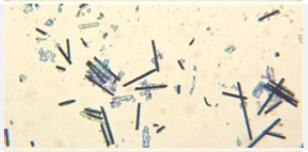 | Central | [36] (0.0612) | | NA | Numerous short to long fibres as well as opaque and transparent dust particles were observed. Relatively, carbon fibres were much more abundant than silica fibres (82%; n = 24.9/image). |
| **A5** $\times 10^{-1}$ | 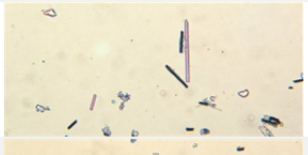 | Personal | [33] (0.0561) | 30 min Sanding HEV12020 | Yes | **Numerous short to long fibres as well as opaque and transparent dust particles were observed. Relatively, carbon fibres were much more abundant than silica fibres (69%; n = 9.25/image).** |
| A6 $\times 10^{-1}$ | 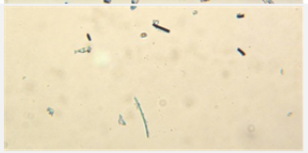 | Background | [39] (0.0663) | | NA | Some generally short fibres and a few longer (only glass-fibres) as well as opaque and transparent dust particles were observed. Relatively, carbon fibers were much more abundant than silica fibres (> 90%; n = 5.5/image). |
| **A17** $\times 10^{-3}$ | 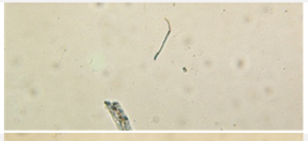 | Personal | [33] (0.0561) | 2 × 12 min Cutting; HEV12025 | Yes | **The sample contains mainly transparent particles, but also some opaque particles and a few very short fibres/fiber fragments were observed. Some particles resemble the dust found during the sanding process.** |
| A3 $\times 10^{-1}$ | 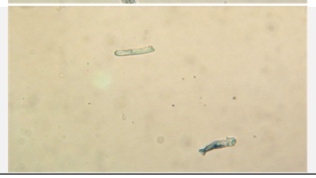 | Outdoor | [315] (0.5365) | all | NA | The sample contains mainly transparent particles, but also some opaque particles were observed. Two fibers assessed as biogenic fibres by means of morphology were observed. |

Since the filter samples were only collected for and sub-divided to allow qualitative microscopy analysis, we cannot determine the absolute quantitative abundance and dimensions of the fibers. However, by count, it appears that the carbon fibers make between 70 and 90% of the total number of fibers in this coarse fraction (Table 3). The fiber diameters are typically between ca 5 and 10 μm, but the lengths are highly variable. The longest observed carbon fiber is ca. 360 μm in length. The longest glass-fiber observed is ca. 210 μm long. However, the typical lengths are considerably shorter, i.e., less than 100 μm. The abundance of these "coarser" and generally long fibers are of potential health concern because their diameters range between 5 and 10 μm that makes them sufficiently fine to be inhalable (AGGIH, 1985). The aerodynamic diameter does not increase significantly with increasing fibre length at given diameters below 4,5, μm respectively. That means that fibres (as well as particles) measured with a diameter below 5 are inhalable. At least for the carbon fibers these characteristics would classify them as long insoluble fibers that may in part reach the alveolar region of the lung.

## DISCUSSIONS

Measured airborne particles and deposited dust samples span a wide size range from 6 nm to several hundred micrometers. To account for their various characteristics, different methods are needed to describe the sampled material. However, airborne exposure particle size range is over several orders of magnitude and therefore the effort in a case study like this is defendable. When entering a new site, we strongly recommend a similar approach before starting workplace monitoring and actions aiming for emission control. In this case, the outdoor particles may have been captured by the online instruments, whereas the fibers, especially the large ones couldnot be measured. On-line instruments give us a good estimate of the exposure (Jensen *et al.*, 2015). However, detailed characterization requires several analysis techniques.

Fibers studied in this case are not in the nano-range; nevertheless, they are respirable and as such they constitute a potential danger to workers' health. Due to the known risk of fibers (e.g., Lippmann, 1990b; Hesterberg and Hart, 2001; Donaldson and Tran, 2004, Skogstad *et al.*, 2006, Føreland *et al.*, 2008, Costa and Orriols, 2012), especially the insoluble ones, investigation of potential release of fibers and their characteristics were of great interest for this study. We describe the nature of fibers (carbon or glass fiber; size; aspect ratio) as fiber toxicity is primarily a function of their concentration, dimension and solubility in the lungs (Lippmann, 1990a; Baron, 2001). SEM and OM results show that fibers are present amongst the micron sized particles, and more dominantly in the micron size range. OM image analyses suggest that carbon fibers are most abundant, despite the fiber mats contained 20–30% carbon fiber and 39–53% glass fiber. This is ascribed to the brittle nature of the glass fibers, breaking down into smaller pieces with aspect ratios smaller than 3. The combination of all EM and OM results allows us to conclude that the occurrence of fibers in the inhalable size range is limited to the production facility and can be directly allocated to the sanding process. Fibers were observed at the location corresponding to near field and far field (Jensen *et al.*, 2015), and also on personal samplers mounted on workers. Thus they do present a potential risk to workers.

One of the key questions in workplace measurements is the discrimination between background particles and process-related particle release (e.g., Ono-Ogasawara *et al.*, 2009, Kuhlbusch *et al.*, 2011; Ramachandran *et al.*, 2011; Vogel *et al.*, 2013; Kaminski *et al.*, 2015). A goal within this study is to identify the different types of particles in the airborne state and discriminate between the process-related sanding dust and a background contribution from potential internal and ambient sources. We identify two different sources (environmental background and sanding dust release) for the aerosol in this facility, but a quantitative source apportionment cannot be provided in the scope of this study. However, the study points out some requirements for adequate exposure assessment.

The 200 nm spherical particles abundant in the TEM samples are ammonium sulfate (as classified by the applied scheme) likely originating from ambient air. The Cryo-TEM results indicate that ammonium sulfate particles (or particles at least dominated by ammonium sulfate) are mixed with a secondary compound that separated during freezing in the TEM (efflorescence, Imre *et al.*, 1997; Cziczo and Abbatt, 1999; Bertram *et al.*, 2011). This mixing may have occurred before the particles entered the production hall, but it is also possible that ammonium sulfates adsorb and mix with semi-volatile compounds, such as styrene or fumes and volatiles released from the epoxy in the workplace atmosphere.

Whereas the environmental contribution in the larger size range might have different sources, the small particle mixing state points towards a polluted environment (Utsunomiya *et al.*, 2002, 2004).

The abrasive treatment of the manufactured composite thus produces particles mainly in the micron and micron size range.

In order to fully characterize the exposure and address potential health effects, we use conventional TEM, Cryo-TEM, unattended SEM and OM for single particle characterization in accordance with the NEAT procedure (Methner *et al.*, 2009, 2010). Furthermore, we show that the classification scheme "Groupp" is valid to be used for classification of particles generated in a work process and helps to identify ambient sources. However, improvements targeted to the application of this scheme on man-made particles and fibers are desirable. The usage of sampling with the MINI impactor has limitations, despite its short sampling times. The sanding peak emissions were actually very short (few seconds), leading to more abundant sampling of background particles by the impactor in the interstitial periods, where the impactor sampling was still ongoing. Timing of sampling can be improved.

It is observed that the characteristics of the deposited dust (Figs. 4 and 5) also give important information on the dusts generated during abrasion and cutting (although

cutting did not show to contribute to a large extent). The particle and fiber sizes of the deposited dust are still in the inhalable to respirable size fraction and contained fibers of concern. Due to their particle sizes, the deposited dust may be easily resuspended into the work room air during vibrations and cleaning and thereby cause a secondary exposure risk. Due to the contents and morphologies of the deposited dust, dermal and inadvertent oral exposure is also of concern. Particles released from composite and breakdown material of fibers appeared to be charging, both in electron microscopy and handling of the material for sample preparation. Charged particles and fibers are observed to stick to the plastic bag; they would thus also stick to plastic material potentially used for separation of the production line, likely causing secondary dermal and inadvertent oral exposure.

The overall abundance of particles and fibers in the production hall is a risk to workers, and this type of exposure demands enforcement of high level respiratory protection from both ultrafine particles and micron to sub-micron fibers. We show that fibers are present not only in the vicinity of the sanding station ("Central", Table 3), but are present all over the production hall ("Personal" and "Background", Table 3). Their distribution and their apparent long residence time, i.e., tens of minutes to hours for micrometer-sized aerosol particles (e.g., Hinds, 2012), in the air is ascribed to the shape of the fibers, which makes the airborne diameter closer to their diameter (width), than their length. If the aerodynamic size is in the inhalable size range, there is no difference between particles and fibers.

## CONCLUSIONS

A combination of measurement techniques allows us to allocate particles in different size ranges to their sources. This work demonstrates that detailed studies are required for adequate exposure assessments.

During sanding and sawing, the factory air was polluted with abrasion dust with a wide size distribution ranging from nm to micron scale dust. Even though the worker used local exhaust control on the sanding device, significant release of the above micron size particles was observed especially to the near-field workplace air (Jensen *et al.*, 2015).

We observe that particles originating from ambient air outside the production hall contribute significantly to the aerosol observed near the working area. Detailed TEM investigations in the small particle size ranges and unattended SEM analysis of micron and super-micron (above micro meter) sized particles prove to be valuable techniques in order to distinguish the particle load caused by an outdoor-contribution and those particles emitted by the abrasive treatment. Furthermore, Cryo-TEM helps avoiding beam damage and rapid evaporation of particles and enables us to investigate and analyse semi-volatile particles and mixtures both structurally and chemically. OM allows us to distinguish carbon and glass fibers, as well as the embedding epoxy material among the inhalable particles.

Fibers are present in the entire size range, but heavily dominate the μm-size fraction. Carbon fibers are most abundant despite the fiber mats containing 20–30% carbon fibers and 39–53% glass fibers which is ascribed to the brittle nature of the glass fibers. The occurrence of fibers in the inhalable size range is limited to the production facility and can be directly allocated to the sanding process.

## ACKNOWLEDGEMENTS

We truly thank Signe H. Nielsen from the National Research Center for the Working Environment for her great job with setting up the sampling equipment. We gratefully acknowledge excellent microscopy conditions at the Center for Electron Nanoscopy (CEN)/Technical University of Denmark, and great technical support by Wilhelmus Huyzer and Dr. Jens Kling. This work was financially supported by a grant from the Danish Centre for Nanosafety (grant agreement N°20110092173/3) by the Danish Working Environment Research Fund. We also like to thank Bodil Holst from the National Research Center for the Working Environment for her help with editing the manuscript.

## REFERENCES

Baron, PA. (2001). Measurement of Airborne Fibers: A Review. *Ind. health* 39: 39–50.

Bello, D., Wardle, B.L., Yamamoto, N., Guzman deVilloria, R., Garcia, E.J., Hart, A.J., Ahn, K., Ellenbecker, M.J. and Hallock, M. (2008). Exposure to Nanoscale Particles and Fibers during Machining of Hybrid Advanced Composites Containing Carbon Nanotubes. *J. Nanopart. Res.* 11: 231–49.

Bertram, A.K., Martin, S.T., Hanna, S.J., Smith, M.L., Bodsworth, A., Chen, Q., Kuwata, M., Liu, A., You, Y. and Zorn, S.R. (2011). Predicting the Relative Humidities of Liquid-Liquid Phase Separation, Efflorescence, and Deliquescence of Mixed Particles of Ammonium Sulfate, Organic Material, and Water Using the Organic-to-Sulfate Mass Ratio of the Particle and the Oxygen-to-Carbon Elemental Ratio of the Organic Component. *Atmos. Chem. Phys.* 11: 10995–1006.

Bugge, M.D., Kjaerheim, K., Foreland, S., Eduard, W. and Kjuus, H. (2012). Lung Cancer Incidence among Norwegian Silicon Carbide Industry Workers: Associations with Particulate Exposure Factors. *Occup. Environ. Med.* 69: 527–533.

Costa, R. aand Orriols, R. (2012) Man-Made Mineral Fibers and the Respiratory Tract. *Arch. Bronconeumol.* 48: 460–468.

Cziczo, D.J. and Abbatt, J.P. (1999). Deliquescence, Efflorescence, and Supercooling of Ammonium Sulfate Aerosols at Low Temperature: Implications for Cirrus Cloud Formation and Aerosol Phase in the Atmosphere. *J. Geophys. Res.* 104: 13781–13790.

Donaldson, K. and Tran, C.L. (2004). An Introduction to the Short-term Toxicology of Respirable Industrial Fibres. *Mutat. Res.* 553: 5–9.

Foreland, S., Bye, E., Bakke, B. and Eduard, W. (2008). Exposure to Fibres, Crystalline Silica, Silicon Carbide and Sulphur Dioxide in the Norwegian Silicon Carbide

Industry. *Ann. Occup. Hyg.* 52: 317–336.

Gomez, V., Levin, M., Saber, A.T., Irusta, S., Dal Maso, M., Hanoi, R., Santamaria, J., Jensen, K.A., Wallin, H. and Koponen, I.K. (2014). Comparison of Dust Release from Epoxy and Paint Nanocomposites and Conventional Products during Sanding and Sawing. *Ann. Occup. Hyg.* 58: 983–994.

Hesterberg, T.W. and Hart, G.A. (2001). Synthetic Vitreous Fibers: A Review of Toxicology Research and its Impact on Hazard Classification. *Crit. Rev. Toxicol.* 31: 1–53.

Hesterberg, T.W., Miiller, W.C., Musselman, R.P. Kamstrup, O., Hamilton, R.D. and Thevenaz, P. (1996) Biopersistence of Man-Made Vitreous Fibers and Crocidolite Asbestos in the Rat Lung Following Inhalation. *Fundam. Appl. Toxicol.* 29: 267–279.

Hinds, WC. (2012) *Aerosol Technology: Properties, Behavior, and Measurement of Airborne Particles*, John Wiley & Sons. ISBN 1118591976.

Imre, D.G., Xu, J., Tang, I.N. and McGraw, R. (1997). Ammonium Bisulfate/Water Equilibrium and Metastability Phase Diagrams. *J. Phys. Chem. A* 101: 4191–4195.

Jensen, A.C.Ø., Levin, M., Koivisto, J., Kling K.I., Saber, A.T. and Koponen, I.K. (2015). Exposure Assessment of Particulate Matter from Abrasive Treatment of Carbon and Glass Fibre-reinforced Epoxy-composites - Two case Studies. *Aerosol Air Qual. Res.* 15: 1906–1916.

Johnsen, H.L., Bugge, M.D., Foreland, S., Kjuus, H., Kongerud, J. and Soyseth, V. (2013). Dust Exposure Is Associated with Increased Lung Function Loss among Workers in the Norwegian Silicon Carbide Industry. *Occup. Environ. Med.* 70: 803–809.

Kaminski, H., Beyer, M., Fissan, H., Asbach, C. and Kuhlbusch, T.A.J. (2015). Measurements of Nanoscale $TiO_2$ and $Al_2O_3$ in Industrial Workplace Environments – Methodology and Results. *Aerosol Air Qual. Res.* 15: 129–141.

Kandler, K. (2009). A Miniature Impactor for Aerosol Collection with Emphasis on Single Particle Analysis. European Aerosol Conference, Karlsruhe, Germany (T092A04).

Kandler, K., Lieke, K., Benker, N., Emmel, C., KÜPper, M., MÜLler-Ebert, D., Ebert, M., Scheuvens, D., Schladitz, A., SchÜTz, L. and Weinbruch, S. (2011). Electron Microscopy of Particles Collected at Praia, Cape Verde, during the Saharan Mineral Dust Experiment: Particle Chemistry, Shape, Mixing State and Complex Refractive Index. *Tellus Ser. B* 63: 475–496.

Koivisto, A.J., Jensen, A.C., Levin, M., Kling, K.I., Maso, M.D., Nielsen, S.H., Jensen, K.A. and Koponen, I.K. (2015). Testing the near Field/Far Field Model Performance for Prediction of Particulate Matter Emissions in a Paint Factory. *Environ. Sci. Processes Impacts* 17: 62–73.

Koponen, I.K., Jensen, K.A. and Schneider, T. (2009). Sanding Dust from Nanoparticle-Containing Paints: Physical Characterisation. *J. Phys. Conf. Ser.* 151: 012048.

Koponen, I.K., Jensen, K.A. and Schneider, T. (2011). Comparison of Dust Released from Sanding Conventional and Nanoparticle-doped Wall and Wood Coatings. *J. Exposure Sci. Environ. Epidemiol.* 21: 408–418.

Kuhlbusch, T.A., Asbach, C., Fissan, H., Gohler, D. and Stintz, M. (2011). Nanoparticle Exposure at Nanotechnology Workplaces: A Review. *Part. Fibre Toxicol.* 8: 22.

Lieke, K., Kandler, K., Scheuvens, D., Emmel, C., Von Glahn, C., Petzold, A., Weinzierl, B., Veira, A., Ebert, M., Weinbruch, S. and SchÜTz, L. (2011). Particle Chemical Properties in the Vertical Column Based on Aircraft Observations in the Vicinity of Cape Verde Islands. *Tellus Ser. B* 63: 497–511.

Lieke, K.I., Rosenørn, T., Pedersen, J., Larsson, D., Kling, J., Fuglsang, K. and Bilde, M. (2013). Micro- and Nanostructural Characteristics of Particles before and after an Exhaust Gas Recirculation System Scrubber. *Aerosol. Sci. Technol.* 47: 1038–1046.

Lippmann, M. (1990a). Effects of Fiber Characteristics on Lung Deposition, Retention, and Disease. *Environ. Health Perspect.* 88: 311–317.

Lippmann, M. (1990b). Man-made Mineral Fibers (MMMF): Human Exposures and Health Risk Assessment. *Toxicol. Ind. Health* 6: 225–246.

Methner, M., Hodson, L. and Geraci, C. (2009). Nanoparticle Emission Assessment Technique (NEAT) for the Identification and Measurement of Potential Inhalation Exposure to Engineered Nanomaterials—Part A. *J. Occup. Environ. Hyg.* 7: 127–132.

Methner, M., Hodson, L., Dames, A. and Geraci, C. (2010). Nanoparticle Emission Assessment Technique (NEAT) for the Identification and Measurement of Potential Inhalation Exposure to Engineered Nanomaterials--Part B: Results from 12 Field Studies. *J. Occup. Environ. Hyg.* 7: 163–176.

Midtgård, U. and Jelnes, J.E. (1991). Toxicology and Occupational Hazards of New Materials and Processes in Metal Surface Treatment, Powder Metallurgy, Technical Ceramics, and Fiber-reinforced Plastics. *Scand. J. Work Environ. Health* 17: 369–379.

Ono-Ogasawara, M., Serita, F. and Takaya, M. (2009). Distinguishing Nanomaterial Particles from Background Airborne Particulate Matter for Quantitative Exposure Assessment. *J. Nanopart. Res.* 11: 1651–1659.

Ramachandran, G., Ostraat, M., Evans, D.E., Methner, M.M., O'Shaughnessy, P., D'Arcy, J., Geraci, C.L., Stevenson, E., Maynard, A. and Rickabaugh, K. (2011). A Strategy for Assessing Workplace Exposures to Nanomaterials. *J. Occup. Environ. Hyg.* 8: 673–685.

Skogstad, A., Foreland, S., Bye, E. and Eduard, W. (2006). Airborne Fibres in the Norwegian Silicon Carbide Industry. *Ann. Occup. Hyg.* 50: 231–240.

Utsunomiya, S., Jensen, K.A., Keeler, G.J. and Ewing, R.C. (2002). Uraninite and Fullerene in Atmospheric Particulates. *Environ. Sci. Technol.* 36: 4943–4947.

Utsunomiya, S., Jensen, K.A., Keeler, G.J. and Ewing, R.C. (2004). Direct Identification of Trace Metals in Fine and Ultrafine Particles in the Detroit Urban Atmosphere. *Environ. Sci. Technol.* 38: 2289–2297.

Vogel, U., Savolainen, K., Wu, Q. Van Tongeren, M. and Brouwer, D. (2013). *Handbook of Nanosafety:*

*Measurement, Exposure and Toxicology*, Elsevier. ISBN 0124166628.

Wentzel, M., Gorzawski, H., Naumann, K.H., Saathoff, H. and Weinbruch, S. (2003). Transmission Electron Microscopical and Aerosol Dynamical Characterization of Soot Aerosols. *J. Aerosol Sci.* 34: 1347–1370.

Wohlleben, W., Brill, S., Meier, M.W., Mertler, M., Cox, G., Hirth, S., von Vacano, B., Strauss, V., Treumann, S., Wiench, K., Ma-Hock, L. and Landsiedel, R. (2011). On the Lifecycle of Nanocomposites: Comparing Released Fragments and Their in-vivo Hazards from Three Release Mechanisms and Four Nanocomposites. *Small* 7: 2384–2395.

Zimmer, A.T. and Maynard, A.D. (2002). Investigation of the Aerosols Produced by a High-speed, Hand-held Grinder Using Various Substrates. *Ann. Occup. Hyg.* 46: 663–672.

*Received for review, May 10, 2015*
*Revised, August 5, 2015*
*Accepted, August 10, 2015*